Clays and Clay Minerals, Vol. 51, No. 6, 701–708, 2003.

EFFECT OF SONICATION ON PARTICLE-SIZE DISTRIBUTION IN NATURAL MUSCOVITE AND BIOTITE

LUIS A. PÉREZ-MAQUEDA[1,*], FRANCISCO FRANCO[2], MIGUEL A. AVILÉS[1], JUAN POYATO[1] AND JOSÉ L. PÉREZ-RODRÍGUEZ[1]

[1] Instituto de Ciencia de Materiales de Sevilla, CSIC-Universidad de Sevilla, C. Américo Vespucio s/n, 41092 Sevilla, Spain
[2] Departamento de Química Inorgánica, Cristalografía y Mineralogía, Facultad de Ciencias, Campus de Teatinos, Universidad de Málaga, 29071 Málaga, Spain

Abstract—The effects of ultrasound treatment on the mean particle size, crystal structure, crystallite dimensions and specific surface area of natural muscovite and biotite samples have been investigated. Sonication of macroscopic flakes of muscovite and biotite produced a drastic particle-size reduction. The conditions for the preparation of micron and submicron-sized muscovite and biotite particles of narrow particle-size distribution by sonochemistry are described. The effect of sonication on particle-size reduction is more significant for muscovite than for biotite. Thus, for long sonication times (100 h), submicron and micron particles are predominant in muscovite and biotite, respectively. The resulting materials are crystalline, as assayed by X-ray diffraction, only broadening of the diffraction lines due to size-reduction was observed. Nuclear magnetic resonance studies revealed that the coordination of Al and Si was not modified by the treatment. Chemical analysis showed that the composition of the sample was not affected by the sonication except for a small contamination by Ti from the tip cup of the sonication instrument.

Key Words—Biotite, Mica, Muscovite, NMR, Particle Size, Sonication, Ultrasound, XRD.

INTRODUCTION

The term mica covers a number of minerals, including 34 different silicates such as muscovite [$(Si_3Al)(Al_2)(OH)_2O_{10}K$] and phlogopite [$(Si_3Al)(Mg_3)(OH)_2O_{10}K$]. Micas are minerals of significant commercial importance due to their physical properties, especially those of brilliance of cleavage faces, cleavage, dielectric strength, elasticity, flexibility, non-conductivity of heat and electricity, resistivity, stability, transparence, *etc*. The commercially important micas are muscovite and biotites. Although biotites have poorer electrical properties than muscovite, biotites have better thermal stability and, therefore, they are used in applications where high-heat stability and electrical properties are required (Harben, 1995; Hedrick, 1999).

Delamination and decrease of the thickness and particle diameter are of interest for the most important applications of mica, especially as filler, anti-sticking and anti-friction powder, lubricant, surface coating, adsorbent, *etc*. One of the most important procedures for particle-size reduction of clays is a mechanical treatment (Somasundaran, 1978; Ovadyahu *et al*., 1998). Grinding of mica can be performed under dry conditions (yielding particles in the range 1.2–150 μm), wet conditions (95–45 μm) or micronized (<53 μm) (Harben, 1995). It has been reported that dry grinding of clays produces progressive amorphization, and yields heterogeneous materials formed of hard agglomerates with modified chemical reactivity (Pérez-Rodríguez *et al*., 1988; Sánchez-Soto *et al*., 1997a, 2000; Temuujin *et al*., 2003). Using wet grinding or steam micronization, it is possible to reduce particle size to the range 90–45 μm. Studies on wet grinding have shown a marked effect of the medium on the characteristics of the ground materials. Papirer *et al*. (1990) observed for muscovite that when the grinding is performed in toluene, the crystalline structure is preserved, while in water or methanol it is destroyed. Those authors also observed that the presence of hydrogen bond-disrupting agents (Li^+, NH_3) facilitates the breakdown of the muscovite structure.

A new technique for delamination and particle-size reduction of clays is sonication. Cavitational collapse sonication on solids leads to microjet and shock-wave impacts on the surface, together with interparticle collisions, which can result in particle-size reduction (Peters, 1996). The effect of ultrasound on vermiculite was studied by Pérez-Maqueda *et al*. (2001) and Pérez-Rodríguez *et al*. (2002). Those workers prepared micron- and submicron-sized vermiculite particles that maintain the structure of the material.

In the present work, the effects of ultrasound on muscovite and biotite are studied extensively. Changes in particle size (as measured by different techniques), structure, crystallite size, specific surface area and chemical composition have been analyzed. Under certain conditions, delamination and relatively narrow particle-size distribution of muscovite and biotite have been obtained.

* E-mail address of corresponding author:
maqueda@cica.es
DOI: 10.1346/CCMN.2003.0510613

EXPERIMENTAL

Material

A muscovite from Sierra Albarrana, (Fuente Obejuna, Córdoba, Spain) and biotite from Santa Olalla (Huelva, Spain) were used as starting materials. The muscovite is a pure mineral and has a half unit-cell composition of $(Si_{3.00}Al_{1.00})(Al_{1.86}Fe^{3+}_{0.15}Mg_{0.04}Ti_{0.03})O_{10}(OH)_2K_{1.00}$. The biotite has a small percentage of Mg-vermiculite (Justo, 1984). Large flakes were ground gently using a Knife-mill (Netzch ZSM-1, Germany) and sieved to <2 mm.

Methods

Sonication. A high-intensity ultrasonic horn that comprises a solid titanium rod connected to a piezoelectric ceramic and a 20 KHz, 750 V power supply was used. The apparatus can be thermostated using a double-jacket reactor. 3 g of <2 mm flakes were mixed with 100 mL of freshly deionized water and subjected to ultrasound for periods ranging from 10 to 100 h.

Specific surface area. The specific surface areas (SSA) were determined with an automatic system (micromeritics 2200 A Model, Norcross GA) at liquid-nitrogen temperature, using the BET method. Nitrogen gas was used as an adsorbate.

Low-angle laser light scattering. The particle-size distribution was determined by low-angle laser light scattering (LALLS, Malvern, Mastersizer model). Measurements were performed in dilute aqueous dispersions (70 mg of sample in 100 mL of water).

X-ray diffraction analysis. Diffraction patterns were obtained using a diffractometer (Kristalloflex D-500 Siemens) at 36 kV and 26 mA with Ni-filtered CuKα radiation and a graphite monochromator. Samples were prepared using a side-packed holder made of aluminum. The holder was tapped with a glass slide cover with a filter paper and filled from the side. The glass covered with the paper was removed before analysis. The dimensions of the coherently diffracting domains (crystallite size) of mica in [001] direction was estimated from the full width at half-maximum (FWHM) of the X-ray diffraction (XRD) peaks using the Scherrer equation.

Scanning electron microscopy. Samples were studied by scanning electron microscopy (SEM) using a Jeol JSM-5400 model. The samples were coated with a thin gold film.

The mean size (length, L) of the particles and the standard deviation (SD) were evaluated from ~100 particles.

Chemical analysis. Chemical analysis was carried out using a sequential X-ray fluorescence spectrometer (Siemens, SRS 3000).

Nuclear magnetic resonance measurements. High-resolution solid-state ^{29}Si and ^{27}Al magic angle spinning (MAS) nuclear magnetic resonance (NMR) spectra of powdered samples were recorded at 79.49 and 104.26 MHz, respectively, in a Bruker MSL-400 spectrometer. Measurements were conducted at room temperature with tetramethylsilane (TMS) and $[Al(H_2O)_6]^{3+}$ as external references.

RESULTS AND DISCUSSION

The chemical analyses of untreated and sonicated muscovite and biotite are shown in Tables 1 and 2,

Table 1. Elemental chemical analysis results (wt.%) (ignition matter basis) for muscovite samples sonicated for different times. Values in brackets correspond to the percentages after correction for Ti contamination.

Sonication time	0 h	10 h	30 h	60 h	100 h
Mg	0.14	0.15 (0.15)	0.18 (0.18)	0.14 (0.14)	0.13 (0.13)
Al	18.62	18.78 (18.85)	18.49 (18.60)	18.21 (18.45)	17.74 (18.37)
Si	21.99	21.82 (21.90)	21.79 (21.92)	21.31 (21.59)	20.16 (20.86)
K	8.69	8.65 (8.68)	8.67 (8.72)	8.61 (8.72)	8.10 (8.38)
Ti	0.05	0.35 (0.05)	0.55 (0.05)	1.25 (0.05)	3.08 (0.05)
Fe	0.85	0.95 (0.95)	0.81 (0.82)	0.92 (0.93)	0.84 (0.86)

Table 2. Elemental chemical analysis results (wt.%) (ignition matter basis) for biotite samples sonicated for different times. Values in brackets correspond to the percentages after correction for Ti contamination.

Sonication time	0 h	10 h	30 h	60 h	100 h
Mg	13.75	13.59 (13.72)	13.39 (13.54)	13.36 (13.50)	13.28 (13.36)
Al	8.78	8.72 (8.80)	8.68 (8.77)	8.60 (8.70)	8.52 (8.66)
Si	17.40	17.32 (17.48)	17.10 (17.30)	17.07 (17.30)	17.08 (17.33)
K	7.01	6.71 (6.78)	6.93 (7.00)	6.91 (7.00)	6.83 (6.98)
Ti	0.25	0.83 (0.25)	0.96 (0.25)	1.2 (0.25)	1.4 (0.25)
Fe	3.43	3.3 (3.4)	3.45 (3.49)	3.48 (3.53)	3.52 (3.56)
Mn	0.11	0.11 (0.11)	0.10 (0.10)	0.12 (0.12)	0.13 (0.13)
Ca	0.12	0.12 (0.12)	0.11 (0.11)	0.12 (0.12)	0.12 (0.12)
Ba	2.20	2.10 (2.12)	2.21 (2.24)	2.21 (2.24)	2.21 (2.24)

https://doi.org/10.1346/CMN.203.0510613 Published online by Cambridge University Press

respectively. For untreated muscovite and biotite, the chemical analyses show equivalent values to those found for these minerals in the literature (Justo, 1984; Newman and Brown, 1987). It is significant from Tables 1 and 2 that the percentages of Ti increase with sonication time in comparison with the untreated samples. This increase is assigned to contamination produced by the tip cup of the sonication equipment. Nevertheless, the percentages of all the other elements, after correcting for the contribution of Ti (Tables 1 and 2, values in brackets), remain unchanged after sonication.

Figure 1 shows the XRD patterns for the samples before and after 100 h of sonication. Sonication does not produce any significant structural alteration, only broadening of the reflections attributed to the delamination and particle-size reduction is observed. The presence of Ti previously detected by chemical analysis is identified in the diffraction pattern as an independent metallic phase.

The ^{29}Si and ^{27}Al MAS-NMR spectra of the muscovite sample before and after 100 h of sonication are included in Figure 2. The ^{29}Si MAS-NMR spectra of both samples show a narrow peak at −85 ppm associated with a Si(Si$_2$Al) environment (Sanz and Serratosa, 1984a; Mackenzie *et al.*, 1987). The ^{27}Al MAS-NMR spectra of these samples contain two resonances, at ~4 and 69 ppm, corresponding to Al in octahedral and tetrahedral sites, respectively (Sanz and Serratosa, 1984b; Mackenzie *et al.*, 1987). These spectra indicate that the coordination of Al and Si are those expected for a muscovite sample and that sonication does not have any effect in the coordination of these two atoms.

The results reported above obtained from chemical analysis, XRD, and MAS-NMR for sonicated samples indicate that the structure is preserved even after long sonication times. These results contrast with those previously reported in the literature for dry-ground silicates. Thus, although for short treatment times, dry grinding of different silicates produces broadening of the XRD reflections due to delamination, progressive treatment produces severe amorphization and smearing of the X-ray lines (Pérez-Rodríguez *et al.*, 1988; Sánchez-Soto *et al.*, 1997, 2000). By ^{29}Si and ^{27}Al MAS-NMR in ground pyrophyllite, tetrahedral sheet breakdown and important modifications in Al coordina-

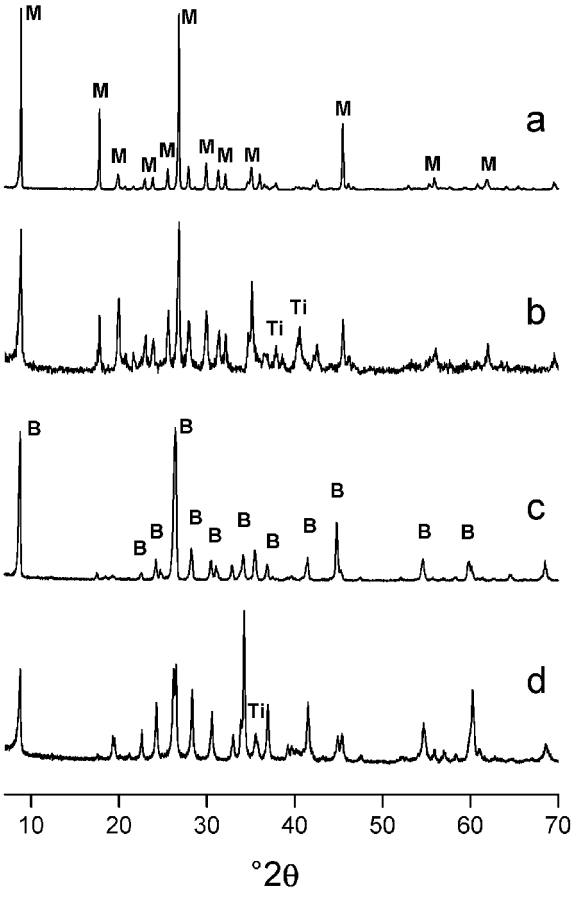

Figure 1. XRD patterns of (a) original muscovite sample, (b) muscovite sample after 100 h of sonication, (c) original biotite sample, (d) biotite sample after 100 h of sonication. B: biotite, M: muscovite and Ti: metallic titanium.

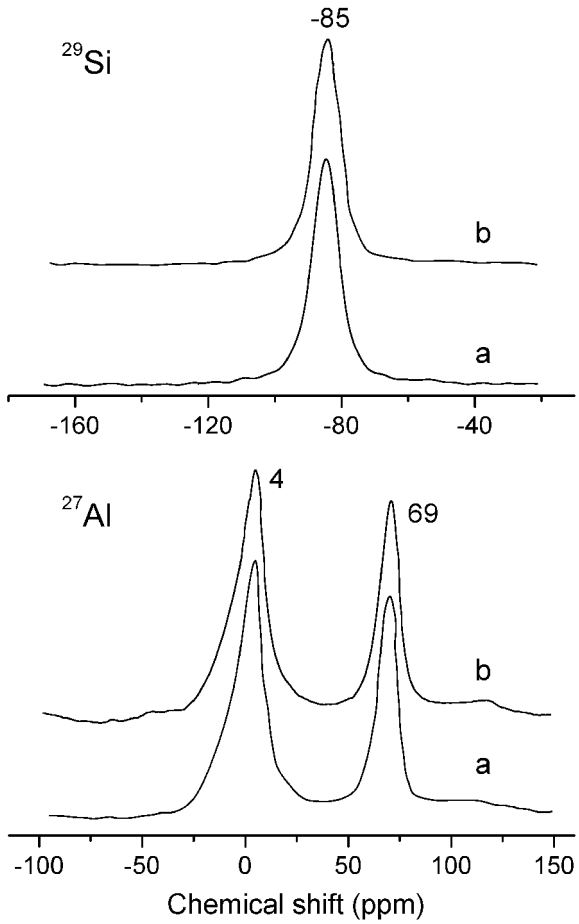

Figure 2. Typical ^{29}Si and ^{27}Al MAS-NMR spectra of muscovite (a) untreated and (b) sonicated for 100 h.

https://doi.org/10.1346/CMN.203.0510613 Published online by Cambridge University Press

tion have been observed (Sánchez-Soto *et al.*, 1997b). On the other hand, Papirer *et al.* (1990) observed that the structure is preserved, as studied by electron diffraction, when grinding is performed in wet conditions with a selected medium (water or methanol in the absence of a hydrogen-bond disrupting agent, *e.g.* Li^+ or NH_3).

The contamination of samples during particle reduction by mechanical treatment is another important issue. It has been noticed previously that grinding introduces significant amounts of contaminants from the grinding media into the samples (Pérez-Rodríguez *et al.*, 1992, 1993). In this work, it has also been observed that sonication produces a small contamination by metallic titanium.

Figures 3 and 4 show the particle-size distribution *vs.* percentage of particle volume at different sonication times of muscovite and biotite, respectively, as estimated by LALLS measurements. The original samples were not measured by LALLS because they consist of large flakes prepared from the macroscopic material by gentle grinding, using a knife-mill, and sieving to <2 mm. Sonicated muscovite samples show a bimodal particle-size distribution. Thus, for the sample sonicated for 10 h (Figure 3a) two modal diameters are observed at 0.57 and 13.71 μm. Increasing sonication time to 20, 40, 60 and 100 h (Figure 3b–e), produces a decrease in the value of the larger modal diameter to 9.80, 6.63, 4.07 and 3.50 μm, respectively, together with a decrease of its volume percentage. However, with the increase in the sonication time, the lower modal diameter remains constant at 0.57 μm while its volume percentage increases. Thus, after 100 h of sonication time, the volume percentage of the small-group particles is much larger than that of the large-group ones.

For biotite (Figure 4), after a sonication period of 10 h, the modal diameter decreases to 20.20 μm, the extreme particles sizes being 1 and 105 μm. On increasing the sonication period, a bimodal distribution is observed. The modal diameter of the large-group particles decreases, reaching values of 13.72, 8.25, 6.15 and 4.96 μm for sonication periods of 20, 40, 60 and 100 h, respectively. The modal diameter of the small-group particles, remains constant at 0.52 μm at the different sonication periods while its volume percentage increases with sonication time.

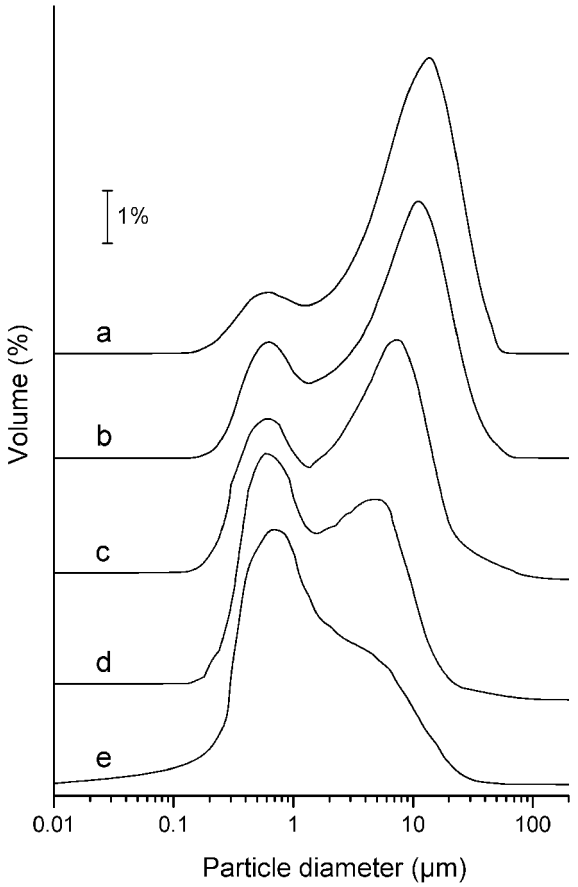

Figure 3. Particle-size distribution (vol.%) for the muscovite sample at different sonication times: (a) 10 h, (b) 20 h, (c) 40 h, (d) 60 h, (e) 100 h.

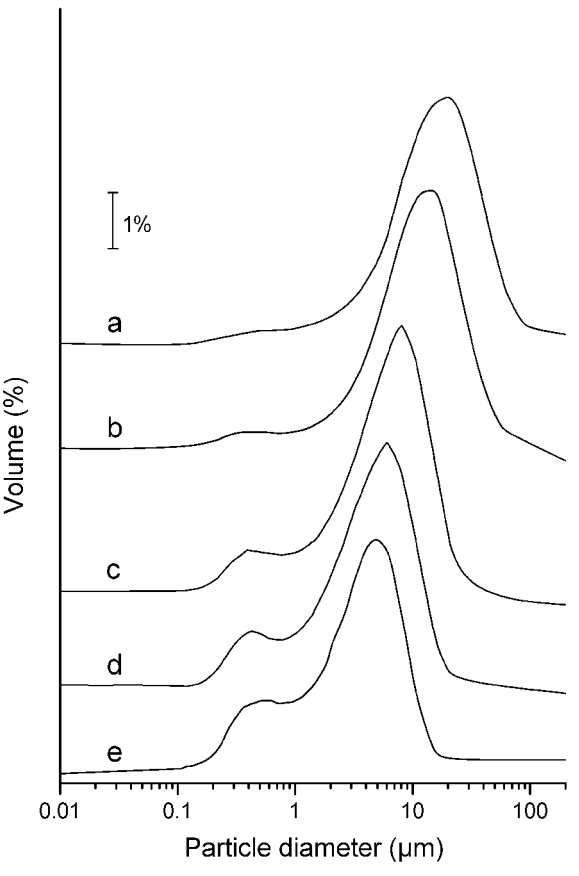

Figure 4. Particle-size distribution (vol.%) for the biotite sample at different sonication times: (a) 10 h, (b) 20 h, (c) 40 h, (d) 60 h, (e) 100 h.

https://doi.org/10.1346/CMN.203.0510613 Published online by Cambridge University Press

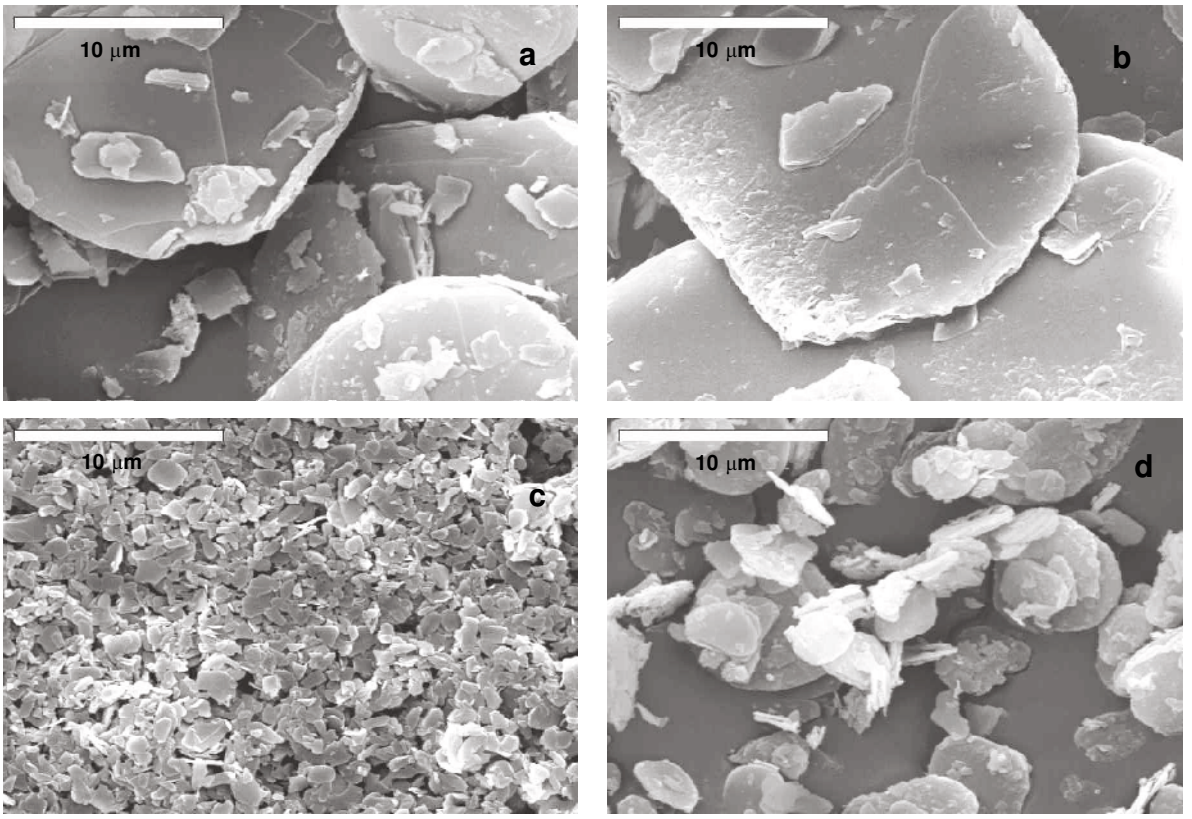

Figure 5. SEM images of the mica samples sonicated for different times: muscovite sonicated for 10 h (a) and 100 h (c); and biotite sonicated for 10 h (b) and 100 h (d). Scale bar: 10 μm.

These LALLS results indicate that sonication produces a significant decrease of the particle-size for both muscovite and biotite samples. Thus, the macroscopic flakes of muscovite and biotite are reduced to micron and submicron particles. The effect of sonication on the particle size is continuous with the treatment time yielding a bimodal particle-size distribution. The modal diameter of the large-group particles decreases with the treatment while its volume percentage decreases. For the small-group particles, the modal diameter remains unchanged with the sonication time, while its volume percentage increases. In general, although the particle sizes of both untreated samples are very similar, sonication has a more marked effect on muscovite than on biotite. When using the same sonication time, the volume percentages of the small-group particles are much larger than those of the corresponding biotite.

The gradual size reduction that occurs during sonication of muscovite and biotite was also revealed by SEM. Some selected micrographs are shown in Figure 5. From the beginning of the sonication treatment (10 h, Figure 5a,b), delamination and particle fracture are observed, producing a notable decrease of the particle size. Longer treatment times produce further delamination and reduction of the particle size, as shown in Figure 5c,d for samples treated for 100 h. It is also clear from these micrographs that sonication produces a more notable particle-size reduction for muscovite than for biotite. For both samples, the sonicated materials consist of very thin plate-like particles.

The evolution of the mean size (length, L) and its standard deviation (SD) with the sonication time are shown in Table 3. For both samples, the mean size decreases with sonication time. Thus, the initial values of original muscovite and biotite, <2 mm, decrease to 4.12 μm and 7.95 μm, respectively, after 10 h of sonication. For biotite, the particle length decreases to 2.38 μm after 100 h of sonication. For muscovite, the decrease in particle size is even more marked, reaching a length of 0.45 μm after 100 h of sonication.

Table 3. Particle length (L) and standard deviation (SD) for sonicated muscovite and biotite samples, as calculated from SEM images.

Sonication time	Muscovite		Biotite	
	L (μm)	SD	L (μm)	SD
10 h	4.12	±5.27	7.95	±6.32
30 h	1.80	±2.21	5.26	±3.91
40 h	0.71	±0.25	4.23	±2.24
50 h	0.52	±0.21	3.29	±3.36
60 h	0.49	±0.21	3.09	±2.27
100 h	0.45	±0.14	2.38	±1.36

https://doi.org/10.1346/CMN.203.0510613 Published online by Cambridge University Press

Additionally, for both samples, it is also worth noting that the SD values decrease with sonication time, indicating that the particle-size distribution becomes narrower with sonication.

Laser-scattering methods do not measure particle sizes in a particular crystallographic direction. The measure of thickness by SEM also presents some difficulties, mainly due to the particle orientation. On the other hand, methods based on the broadening of the XRD peaks average diffraction effects from a large number of individual crystallites and give information on dimensions in a crystallographic direction. Besides, these sizes are related to microdomains of coherent scattering and not to agglomerates. Figure 6 shows the evolution with the sonication time of the crystallite size, as calculated by the Scherrer broadening method using the 001 reflection. This is a basal reflection and may be used for a direct estimate of the particle thickness. These results show very different behavior for both samples. Thus, muscovite suffers a sharp decrease in its crystallite size for up to 40 h of treatment time, remaining almost unchanged for longer treatment times. On the other hand, biotite suffers a smooth and continuous delamination throughout the entire sonication time range studied. For treatment times <33 h, muscovite has a larger crystallite size than biotite, while for treatment times >33 h, the situation is just the opposite. Delamination has been also reported for other phyllosilicate minerals on grinding, but amorphization has also been reported when increasing the treatment times (Pérez-Rodríguez *et al.*, 1988). Nevertheless, muscovite and biotite samples sonicated for up to 100 h are still crystalline according to the XRD study (Figure 1); only broadening of the peaks which could be attributed to the delamination and crystallite-size reduction, has been observed.

The evolution of specific surface area (SSA) with sonication time is shown in Figure 7, which shows a similar behavior for both samples up to 40 h. In this time range, the SSA increases to ~26 m^2g^{-1}. For sonication times >40 h, the evolution of the SSA of both samples is quite different. Thus, up to 100 h of sonication time, biotite continues the same initial trend, showing a steady growth with the sonication time. For 100 h of sonication time, the resulting SSA is 45 m^2g^{-1}. On the other hand, the muscovite sample shows a levelling off for sonication times >40 h, yielding an SSA of 29 m^2g^{-1} for 100 h of sonication time.

The SSA values are larger for biotite than for muscovite for sonication times >40 h; nevertheless, the other experimental methods used in this work for measuring particle size (SEM, LALLS and broadening of XRD peaks) show smaller particle sizes for muscovite than for biotite. These apparently contradictory results might be attributed to the presence of some impurities of vermiculite in the biotite sample. Thus, Pérez-Maqueda *et al.* (2001) found that sonication of vermiculite produces higher SSA values than those expected for only a decrease in the particle size. This excess in specific surface area for vermiculite can be attributed to the fact that N_2 penetrates between the individual layers of vermiculite (Thomas and Bohor, 1969). Therefore, in vemiculites, the BET surface is not only external but there is some contribution by the interlayer. Another important parameter that should be considered is the weathering of these two samples. Thus, the biotite sample is more weathered than the muscovite, as indicated by the presence of vermiculite and a smaller percentage of K. This weathering produces frayed edges (Fanning and Keramidas, 1977) that may have an influence on the N_2 adsorption.

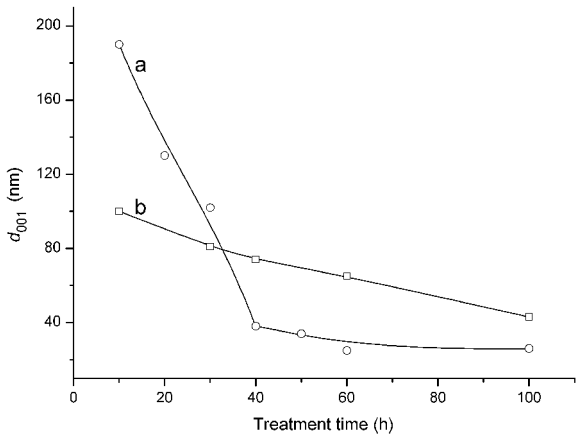

Figure 6. Evolution of the crystallite size (D_{001}), as calculated by the Scherrer broadening method using the 001 reflection, with the sonication time; (a) muscovite and (b) biotite.

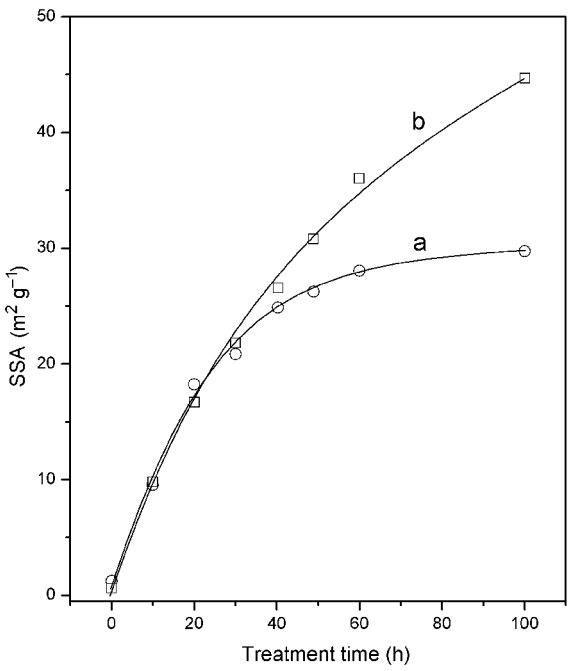

Figure 7. Evolution of the specific surface area (SSA) with sonication time for: (a) muscovite and (b) biotite.

https://doi.org/10.1346/CMN.203.0510613 Published online by Cambridge University Press

The results included in this work on the particle-size reduction of mica by sonication indicate that sonication produces a sharp decrease in particle size while retaining the characteristic plate-like shape of the phyllosilicates. The resulting material presents a relatively narrow particle-size distribution and it is free of aggregates. These results contrast with those reported for dry grinding of clays. Thus, dry grinding produces particle-size reduction, but the shape changes yielding heterogeneous, scarcely aggregated, particles (Pérez-Rodríguez *et al*., 1988; Sánchez-Soto *et al*., 1997a, 2000, Temuujin *et al*., 2003). Papirer *et al*. (1990) observed that wet grinding preserves the laminar shape of the muscovite precursors, but no studies have been presented on the particle size and particle-size distribution of the products.

CONCLUSIONS

Particle-size analysis by LALLS of sonicated mica flakes showed that increasing sonication time causes a decrease in particle size with two kinds of particles appearing, one with an average particle size in the micron range and the other in the submicron range. The volume percentage of the former decreases while that of latter increases. The SEM images of sonicated muscovite and biotite showed that the samples consist of plate-like particles. A gradual reduction of particle size is detected with increasing sonication time. The crystallite size in the basal direction [001] of both samples indicates important delamination with sonication. All these methods show that particle-size reduction is more notable for the muscovite than for the biotite samples studied here.

X-ray diffraction studies indicate that, even after 100 h of sonication time, mica is not amorphized and the crystalline structure is not damaged. The NMR studies reveal that the coordination of Si and Al is not modified by the sonication treatment. Chemical analyses also show similar compositions for sonicated and untreated samples, with only a small increase in titanium observed, attributed to contamination produced by the tip cup of the sonication equipment. All the above results indicate that sonication of macroscopic muscovite and biotite flakes yields micron and submicron plate-like crystalline particles without significant structural damage.

Sonication is a feasible procedure for particle-size reduction of mica samples while preserving the crystalline structure, and yielding plate-like particles with a relatively narrow particle-size distribution and free of aggregation.

ACKNOWLEDGMENTS

Financial support from The Spanish Ministry of Research and Development through grant MAT2002-03774 is gratefully acknowledged.

REFERENCES

Fanning, D.S. and Keramidas V.Z. (1977) Micas. Pp. 195–258 in: *Minerals in Soil Environments* (J.B. Dixon and S.B. Weed, editors). Soil Science Society of America, Madison, Wisconsin.

Harben, P.W. (1995) *The Industrial Minerals Handbook*. Industrial Minerals Division. Metal Bulletin plc, London.

Hedrick, J.B. (1999) Mica. *American Ceramic Society Bulletin*, **78**, 136–138.

Jackson, M.L. (1975) *Soil Chemical Analysis– Advanced Course*, 2nd edition. Published by the author, Madison, Wisconsin.

Justo, A. (1984) Estudio Fisicoquímico y Mineralógico de Vermiculitas de Andalucía y Badajoz. PhD thesis. Universidad de Sevilla, Sevilla, Spain.

Mackenzie, K.J.D., Brown, I.W.M., Cardile, C.M. and Meinhold, R.H. (1987) The thermal reactions of muscovite studied by high-resolution solid-state 29-Si and 27-Al NMR. *Journal of Materials Science*, **22**, 2645–2654.

Newman, A.C.D. and Brown, G. (1987) The chemical constitutions of clays. Pp 1–128 in: *Chemistry of Clays and Clay Minerals* (A.C.D. Newman, editor). Monograph **6**. Mineralogical Society, London.

Ovadyahu, D., Yariv, S., Lapides, I. and Deutsch, Y. (1998) Mechanochemical adsorption of phenol by tot swelling clay minerals. II Simultaneous DTA and TG study. *Journal of Thermal Analysis and Calorimetry*, **51**, 431–447.

Papirer, E., Eckardt, A., Muller, F. and Yvon, J. (1990) Grinding of muscovite, influence of the grinding medium. *Journal of Materials Science*, **25**, 5109–5117.

Pérez-Maqueda, L.A., Caneo, O.B., Poyato, J. and Pérez-Rodríguez, J.L. (2001) Preparation and characterization of micron and submicron-sized vermiculite. *Physics and Chemistry of Minerals*, **28**, 61–66.

Pérez-Rodríguez, J.L., Madrid, L. and Sánchez-Soto, P.J. (1988) Effect of dry grinding on pyrophyllite. *Clay Minerals*, **23**, 399–410.

Pérez-Rodríguez, J.L., Pérez-Maqueda, L.A., Justo, A. and Sánchez-Soto, P.J. (1992) Influence of grinding contamination on high temperature phases of kaolinite. *Industrial Ceramics*, **12**, 109–113.

Pérez-Rodríguez, J.L., Pérez-Maqueda, L.A., Justo, A. and Sánchez-Soto, P.J. (1993) Influence of grinding contamination on high temperature phases of pyrophyllite. *Journal of the European Ceramics Society*, **11**, 335–339.

Pérez-Rodríguez, J.L., Carrero, F., Pérez-Maqueda, L.A. and Poyato, J. (2002) Sonication as a tool for preparing nanometric vermiculite particles. *Nanotechnology*, **13**, 382–387.

Peters, D. (1996) Ultrasound in materials chemistry. *Journal of Material Chemistry*, **6**, 1605–1618.

Sánchez-Soto, P.J., Wiewióra, A., Aviles, M.A., Justo, A., Pérez-Maqueda, L.A., Pérez-Rodríguez, J.L. and Bylina, P. (1997a) Talc from Puebla de Lillo, Spain. II. Effect of dry grinding on particle size and shape. *Applied Clay Science*, **12**, 297–312.

Sánchez-Soto, P.J., Pérez-Rodríguez, J.L., Sobrados, I. and Sanz, J. (1997b) Influence of grinding in pyrophyllite-mullite thermal transformation assessed by ^{29}Si and ^{27}Al MAS NMR spectroscopies. *Chemistry of Materials*, **9**, 677–684.

Sánchez-Soto, P.J., Jiménez de Haro, M.C., Pérez-Maqueda, L.A., Varona, I. and Pérez-Rodríguez, J.L. (2000b) Effects of dry grinding on the structural changes of kaolinite powders. *Journal of the American Ceramic Society*, **83**, 1649–1657.

Sanz, J. and Serratosa, J.M. (1984a) Si-29 and Al-27 high-resolution MAS-NMR spectra of phyllosilicates. *Journal of*

the American Chemical Society, **106**, 4790–4793.
Sanz, J. and Serratosa J.M. (1984b) Distinction of tetrahedrally and octahedrally coordinated Al in phyllosilicates by NMR-spectroscopy. *Clay Minerals*, **19**, 113–115.
Somasundaran, A. (1978) Theories of grinding. Pp. 105–124 in: *Ceramic Processing Before Firing* (G. Onada and L. Mench, editors). Wiley, New York.
Temuujin, J., Okada, K., Jadambaa, T.S., MacKenzie, K.J.D. and Amarsanaa, J. (2003) Effect of grinding on the leaching behaviour of pyrophyllite. *Journal of the European Ceramic Society*, **23**, 1277–1282.
Thomas, J., Jr, and Bohor, B.F. (1969) Surface area of vermiculite with nitrogen and carbon dioxide as adsorbates. *Clays and Clay Minerals*, **17**, 205–209.

(*Received 21 March 2003; revised 4 August 2003; Ms. 774*)